Building synthetic acoustic spectra: theory and pipeline of matlab routines

H-C. Nataf [1]

ISTerre Geodynamo team

September 21, 2019, version 2

I recall here the theories used to infer the acoustic modes of our ZoRo experiment and predict synthetic spectra. In this note, I also present the pipeline of matlab routines I have written to compute and plot these spectra, and compare them with measured spectra.

Version 2 corrects several errors that were present in the literature, and adds more references. The modifications concern:

- bulk viscosity μ_b: its contribution to bulk attenuation was written as $\frac{1}{2}\mu_b$ in Moldover et al. (1986), and in some of his later publications. The $\frac{1}{2}$ factor is erroneous (see Guianvarc'h et al. (2009) for example). I have thus corrected equation 27. I have also collected and added values of bulk viscosity for all gases and liquids proposed in my programs. Note that Hu et al. (2015) claim that γ instead of $(\gamma - 1)$ should be used in that same equation. Jordan and Keiffer (2016) demonstrate that this is not true.
- figure for Ledoux coefficients: I replaced the l-scaling factor I was using by $(l + 1)$ since it was erroneously suggesting zero effect for $l = 0$.
- ellipticity correction: this part has turned into a big thing, which I have transferred to a separate file entitled: Notes_ellipticity_pipeline. The corresponding functions are gathered in the ellipticity_library folder.

1. Theory of acoustic modes in a spherical shell of fluid enclosed between two spherical elastic shells

1.1. rigid shell and no inner sphere

The starting point is the theory for acoustic modes in a sphere of a compressible fluid with an outer rigid boundary and no inner sphere. From the fundamental law of dynamics and thermodynamics, one gets the following wave equation governing the pressure $P(\mathbf{r}, t)$ in an isentropic fluid (Triana et al., 2014):

$$\frac{\partial^2}{\partial t^2} P(\mathbf{r}, t) = c^2 \nabla^2 P(\mathbf{r}, t), \tag{1}$$

where c is the sound speed. Assuming an oscillatory time dependence, $P(\mathbf{r}, t) = f(\mathbf{r})\, \mathrm{e}^{-\mathrm{i}\omega t}$, then $f(\mathbf{r})$ obeys the Helmholtz equation:

$$\nabla^2 f(\mathbf{r}) + k^2 f(\mathbf{r}) = 0, \tag{2}$$

[1] email: Henri-Claude.Nataf@univ-grenoble-alpes.fr

where $k = \omega/c$ is the wave number. The Helmholtz equation is separable in spherical coordinates so that $f(\mathbf{r}) = R(r)\,\Theta(\theta)\,\Phi(\varphi)$. The solutions for the θ and φ equations are the spherical harmonics $Y_l^m(\theta,\varphi) = P_l^m(\cos\theta)\,\mathrm{e}^{im\varphi}$, where l is the angular degree, which corresponds to the number of nodes in the angular coordinates, while m is the azimuthal order (the number of nodes in the azimuthal direction). The radial equation is:

$$\frac{\partial}{\partial r}\left[r^2\frac{\partial}{\partial r}R(r)\right] = \left[l(l+1) - k^2r^2\right]R(r). \tag{3}$$

The solution for $R(r)$ is a sum of spherical Bessel functions, which reads, apart from a normalizing factor,

$$R(r) = j_l(kr) + B\,y_l(kr), \tag{4}$$

where $j_l(x)$ and $y_l(x)$ are the spherical Bessel functions of degree l of the first and second kind, respectively.

In the absence of an inner sphere, the solution only involves the spherical Bessel function of the first kind:

$$R(r) = j_l(kr). \tag{5}$$

The fluid displacement vector $\zeta(\mathbf{r})$ is related to the fluid pressure by Euler's equation, yielding:

$$\zeta(\mathbf{r}) = \zeta_r(\mathbf{r})\hat{\mathbf{r}} + \zeta_h(\mathbf{r}) = \frac{\nabla P(\mathbf{r})}{\rho_f\,\omega^2}, \tag{6}$$

where ρ_f is the density of the fluid. Replacing $P(\mathbf{r})$ by its expression, we get the radial ζ_r and horizontal ζ_h components of the displacement as:

$$\zeta_r(\mathbf{r}) = \frac{1}{\rho_f\,\omega^2}\,\xi_r(r)P_l^m(\cos\theta)\,\mathrm{e}^{\mathrm{i}m\varphi} \tag{7}$$

$$\zeta_h(\mathbf{r}) = \frac{1}{\rho_f\,\omega^2}\,\xi_h(r)\left[\frac{d}{d\theta}P_l^m(\cos\theta)\,\hat{\theta} + \mathrm{i}\frac{\mathrm{m}}{\sin\theta}\mathrm{P}_\mathrm{l}^\mathrm{m}(\cos\theta)\,\hat{\varphi}\right]\mathrm{e}^{\mathrm{i}m\varphi}, \tag{8}$$

with the radial functions $\xi_r(r)$ and $\xi_h(r)$ of the radial and horizontal displacement components respectively given by:

$$\xi_r(r) = R'(r) \tag{9}$$

$$\xi_h(r) = \frac{R(r)}{r} \tag{10}$$

The presence of the spherical rigid outer boundary at $r = r_o$ quantifies the wave number. Indeed, the radial displacement should vanish there, implying $R'(r_o) = 0$. Hence, for each l degree, only those wave numbers ${}_nk_l$ that satisfy $d\,j_l({}_nk_l\,r)/dr = 0$ at $r = r_o$ yield acoustic modes. The index n corresponds to the number of nodes in the radial direction. Following the seismological notation, we will note ${}_nS_l^m$ an acoustic mode of angular degree l, order m, and radial degree n. Note that length is normalized by r_o in our computations, so that the ${}_nk_l$ wave number mentioned above is dimensionless.

One can thus get the frequencies ${}_nf_l$ of all the needed acoustic modes by scanning all l from 0 to some l_{max} value, then solving for all ${}_nk_l$ wave numbers that satisfy the boundary condition, thus obtaining:

$${}_nf_l = \frac{c\,{}_nk_l}{2\pi r_o}. \tag{11}$$

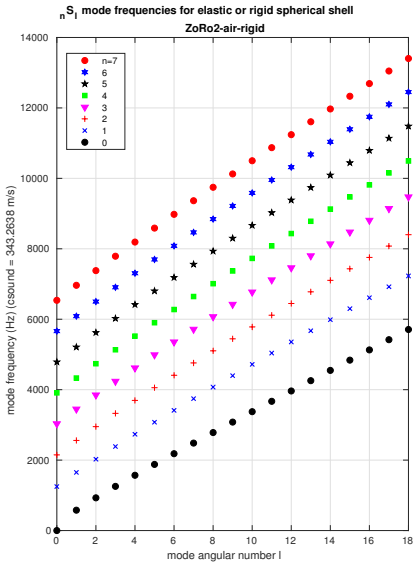

Figure 1: frequencies ${}_nf_l$ of degenerate ${}_nS_l$ multiplets as a function of angular degree l and radial degree n in the ZoRo2 experiment filled with air, assuming a rigid outer wall.

Figure 1 displays the frequencies of the acoustic modes computed for ZoRo2. It is important to realize that the m order does not appear in this expression: the ${}_nS_l^m$ acoustic modes are degenerate in m. Several elements break this degeneracy, and in particular flow in the fluid: this is the key of the 'modal acoustic velocimetry' technique we are using.

1.2. rigid shell and rigid inner sphere

One can easily add a rigid inner sphere of radius r_i, as described in Triana et al. (2014). We then need to keep the $B\,y_l(kr)$ in equation 4 and add a new boundary condition $R'(r_i) = 0$. For each acoustic modes, we now get its wave number ${}_nk_l$ and the corresponding ${}_nB_l$ coefficient for B, which yields the amplitude of the y_l term with respect to the j_l term.

1.3. elastic shell and no inner sphere

The theory is adapted from the article by Rand and DiMaggio (1967), entitled 'Vibrations of Fluid-Filled Spherical and Spheroidal Shells'. Here, the 'shell' is the elastic wall containing the fluid; there is no inner sphere in that study. Dealing with an elastic shell implies adding a momentum equation for that shell, and an equation that states that the fluid radial velocity equates the shell radial velocity at the surface of the fluid.

The elasticity of the shell is described in terms of its shear modulus μ and Poisson's ratio ν. It is h-thick and its density is ρ. We also need the fluid density ρ_f and its sound speed c. In addition to the fluid pressure $P(\mathbf{r}, t)$, the radial displacement $U(\theta, t)$ and tangential displacement $W(\theta, t)$ of the shell are introduced, in a thin shell approximation. Note that the treatment assumes these are axisymmetric and non-torsional.

Here, we only consider the spherical case. Since acoustic modes are degenerate in this problem as well, results obtained for $m = 0$ also apply to $m \neq 0$.

Then, calling $\eta = \cos\theta$, the governing equations are the equations (13-17) of Rand and DiMaggio (1967):

$$-\sin\theta\frac{d^2U\sin\theta}{d\eta^2} - (1-\nu)U - (1+\nu)\sin\theta\frac{dW}{d\eta} - \frac{1-\nu}{2}\frac{\rho r_o^2\omega^2}{\mu}U = 0 \tag{12}$$

$$(1+\nu)\frac{dU\sin\theta}{d\eta} + 2(1+\nu)W - \frac{1-\nu}{2}\frac{\rho r_o^2\omega^2}{\mu}W = \frac{1-\nu}{2}\frac{r_o^2}{h\mu}P(r_o,\cos\theta) \tag{13}$$

$$W = \frac{1}{\omega^2\rho_f}\frac{\partial P}{\partial r}(r_o,\cos\theta) \tag{14}$$

$$\frac{\partial}{\partial\eta}\left[\sin^2\theta\frac{\partial P}{\partial\eta}\right] + \frac{\partial}{\partial r}\left(r^2\frac{\partial P}{\partial r}\right) + \frac{\omega^2}{c^2}r^2P = 0 \tag{15}$$

$$U(\pm1) = 0. \tag{16}$$

Rand and DiMaggio (1967) demonstrate that these equations can be cast into a single equation in P only, to be satisfied at $r = r_o$ (their equation 18):

$$g_1P_{\eta\eta r} + g_2P_{\eta r} + g_3P_r + g_4P_{\eta\eta} + g_5P_\eta + g_6P = 0, \tag{17}$$

where P_η denotes $\frac{\partial P}{\partial\eta}$, and so on. Since the angular part is again solved by the spherical harmonics $Y_l^m(\theta,\varphi)$, one gets an equation for the wave number ${}_nk_l$. The expressions for the g_i are given in equations A25-A30 of their article. Note that, the properties of the shell and fluid only enter as ν and the dimensionless λ and κ_0 combinations given by:

$$\lambda = \frac{\rho_f}{\rho}\frac{r_o}{h} \tag{18}$$

$$\kappa_0 = \frac{\rho c^2}{2\mu}. \tag{19}$$

I have coded all this in the elastic_spherical_shell_modes.m routine. The main motivation is that one can estimate the ratio between fluid pressure beneath the outer shell and the outer shell acceleration in a consistent way from equation 14 above (equation 15 of Rand and DiMaggio (1967)). Remember that $\frac{\partial P}{\partial r} = 0$ for a rigid boundary.

1.4. elastic shell and elastic inner sphere

To be complete, I extended the theory of Rand and DiMaggio (1967) to the case of an added elastic inner shell, combining the elements of sections 1.2 and 1.3.

1.5. matlab programs

The elastic_spherical_shell_modes.m function provides the ${}_nk_l$ and ${}_nB_l$ solutions of the general problem, in the shape of $(n = 0 : n_{max}, l = 0 : l_{max})$ arrays. It also returns the corresponding ${}_nf_l$ mode frequency array, given the sound speed c. The input parameters indicate whether there is an inner sphere or not, and provide the required elastic parameters of the elastic shells. For a rigid shell, one simply specifies an infinite shear modulus μ, which yields a zero λ coefficient.

Most relevant routines are placed in the 'acoustic_library' folder. Note that it is important to write as functions all terms that have to be integrated, such as i_nlm. Similarly for terms that enter a function for which we seek the zeroes, such as f_sphere in elastic_sperical_shell_modes.m.

1.5.1. matlab script

- compute_modes_menu.m: this script proposes several spherical shell configurations corresponding to our actual experiments, several fluids relevant for these experiments, and the treatment of the walls (elastic or rigid). From these elements, it computes the degenerate ${}_nS_l$ acoustic modes and their properties. It proposes to plot the resulting mode frequencies and coefficients (Acc, ${}_n\gamma_l$, ${}_ndk2_l^m$, ${}_nC_l$, ${}_ng_l$), and to save all these, together with the ${}_nk_l$, ${}_nB_l$ and ${}_nf_l$ arrays. The name of the mode file is built as 'ZoRo2-air-rigid.mat' for example.

1.5.2. matlab functions

- elastic_spherical_shell_modes.m: computes the mode wave numbers (and frequencies) and 'B' factors of degenerate ${}_nS_l$ modes of a spherical fluid shell between elastic walls. The walls can also be rigid, and there can be no inner sphere.
- gas_properties.m: provides the needed thermodynamic properties of various gases as a function of pressure and temperature.
- acceleration_coefficient.m: computes the acceleration to pressure ratio at the outer wall for degenerate ${}_nS_l$ modes.
- write_acoustic_modes.m: writes a 'mat' file containing the wave numbers, frequencies, 'B' factors and resulting coefficients (Acc, ${}_n\gamma_l$, ${}_nC_l$, ${}_ng_l$, ${}_n\Delta f_l$) for degenerate ${}_nS_l$ modes of a given shell configuration.
- read_acoustic_modes.m: reads the mode 'mat' file.
- A_nlm.m: computes the ${}_nA_l^m(r,\theta)$ meridional map of acoustic pressure amplitude of ${}_nS_l^m$ modes in a spherical shell.

1.5.3. drawing functions

Drawing routines are gathered in the 'drawing_functions' folder.

- draw_elastic_modes.m: plots the frequencies ${}_nf_l$ of the ${}_nS_l$ modes as a function of angular degree l for all available n.
- draw_acceleration_ratios.m: plots the acceleration ratios Acc of the ${}_nS_l$ modes as a function of angular degree l for all available n.

2. Mode splitting due to rotation

Several deviations from our original assumptions can lift the m-degeneracy of ${}_nS_l^m$ acoustic modes. When these deviations are not too large, they can be treated as perturbations of the spherical ${}_nS_l^m$ modes, which has the advantage to keep the well-defined sequence of modes. This is what is most often done in seismology, where the ${}_nS_l^m$ and ${}_nT_l^m$ (for the toroidal modes) of the SNREI[2] Earth are taken as starting points for various perturbations (Dahlen and Tromp, 1998).

[2]Spherical Non Rotating Elastic Isotropic

We will examine here the perturbations brought by the rotation of the fluid. Perturbations brought by the ellipticity of its container are treated in the separate Notes_ellipticity_pipeline package.

2.1. the effect of global rotation

Concerning rotation, it is important to realize that there are two different effects. When helioseismologists analyze acoustic modes of the Sun, they observe it from the Earth, which means that they examine a rotating object. Acoustic waves that propagate in the Sun in its rotation direction have a higher frequency on its side approaching the Earth, due to the Doppler effect, while the opposite holds for waves propagating in the opposite direction. This effect results in the 'splitting' of the ${}_nS_l$ degenerate 'multiplet' into $2l+1$ 'singlets' ${}_nS_l^m$, whose individual frequencies are ${}_nf_l^m = {}_nf_l + m\,f_o$, where f_o is the rotation frequency of the object (here the Sun).

When seismologists analyze seismic modes of the Earth, their seismometers and the earthquake sources rotate with the Earth. Thus, the effect mentioned above does not take place. However, the rotation of the Earth also induces a splitting, due to the Coriolis force. This splitting is also proportional to m and to f_o, but with a coefficient ${}_nC_l$, called the Ledoux coefficient, which depends upon n and l, so that: ${}_nf_l^m = {}_nf_l - m\,{}_nC_l\,f_o$. The expression of the Ledoux coefficient is given in Aerts et al. (2010, equation (3.361)):

$$ {}_nC_l = \frac{\int_{r_i}^{r_o} \left[2\,\xi_r\,\xi_h + \xi_h^2\right] r^2 dr}{{}_nI_l}, \tag{20} $$

with the normalizing integral:

$$ {}_nI_l = \int_{r_i}^{r_o} \left[\xi_r^2 + l(l+1)\,\xi_h^2\right] r^2 dr, \tag{21} $$

assuming here a homogeneous fluid density.

The Ledoux coefficients computed for ZoRo2 are shown in Figure 2. Note that the correction needs to be performed to the second order for the Earth, because this second order correction has a magnitude similar to the ellipticity correction (Dahlen, 1968). The second order correction involves both an effect of the centrifugal acceleration and a second order Coriolis term.

In our ZoRo experiments, the loudspeakers and microphones are attached to the solid outer shell and rotate with it. Therefore, when both the shell and the fluid rotate uniformly in solid body rotation, splitting will only be due to the Coriolis effect given by the Ledoux coefficients.

2.2. the effect of differential fluid rotation

Remember that we are doing all that to try to infer fluid motions in the rotating sphere! Indeed, axisymmetric azimuthal motions of the fluid also produce a splitting of the degenerate multiplets. The theory, adapted from helioseismology (Aerts et al., 2010), is recalled in Triana et al. (2014).

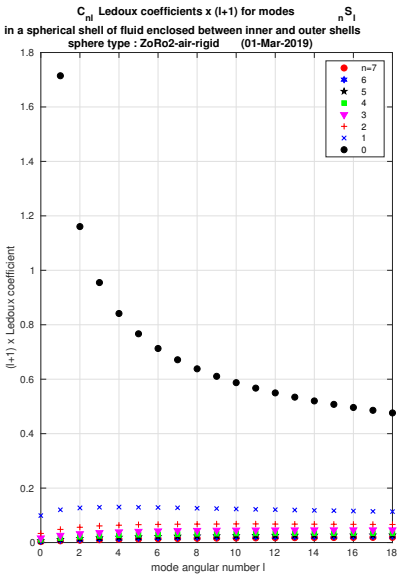

Figure 2: Ledoux coefficients ${}_nC_l$ (times l) of degenerate ${}_nS_l$ multiplets as a function of angular degree l and radial degree n in the ZoRo2 experiment filled with air, assuming a rigid outer wall.

Defining the fluid angular velocity $\Omega(r,\theta)$, the frequency splitting ${}_n\Delta_l^m = {}_nf_l^m - {}_nf_l$ is again proportional to m, but with a coefficient that depends upon m and is obtained by integration of a 'rotational kernel' ${}_nK_l^m(r,\theta)$ such that:

$$ {}_n\Delta_l^m = \int_{r_i}^{r_o}\int_o^{\pi} {}_nK_l^m(r,\theta)\,\Omega(r,\theta)\,r\,dr\,d\theta. \tag{22}$$

defining $p(\theta)$ as the *fully normalized* associated Legendre polynomial of degree l and order m:

$$ p(\theta) = P_l^m(\cos\theta), \tag{23}$$

and its derivative:

$$ q(\theta) = \frac{d}{d\theta}P_l^m(\cos\theta), \tag{24}$$

we obtain the following expression for the rotational kernel:

$$ {}_nK_l^m(r,\theta) = \frac{r\sin\theta}{{}_nI_l}\left\{\xi_r^2p^2 + \xi_h^2\left[q^2 + \frac{m^2}{\sin^2\theta}p^2 - 2\frac{pq}{\tan\theta}\right] - 2\xi_r\,\xi_h p^2\right\}. \tag{25}$$

Note that global solid body rotation of the fluid with respect to the shell, as treated earlier, can be seen as a special case of this more general derivation.

2.3. matlab functions

Most relevant functions are placed in the 'acoustic_library' folder.

- Ledoux_coefficient.m: computes the Ledoux coefficient ${}_nC_l$ of degenerate ${}_nS_l$ modes for global rotation.
- K_nlm.m: computes the ${}_nK_l^m$ rotational kernel of ${}_nS_l^m$ modes for axisymmetric fluid angular velocity.

2.3.1. Drawing functions

- draw_Ledoux_coefficients.m: plots the Ledoux coefficients ${}_nC_l$ of the ${}_nS_l$ modes as a function of angular degree l for all available n.

2.3.2. Lower level functions

- i_nlm.m: integrand of the normalization integral ${}_nI_l$ used for the rotational kernels and ellipticity correction.
- Int_nlm.m: ${}_nI_l$ normalization integral (numerical integration between r_i and r_o of the integrand function i_nlm.m).
- xi_r.m: radial displacement function $\xi_r(r)$ of fluid for degenerate ${}_nS_l$ mode.
- xi_h.m: horizontal displacement function $\xi_h(r)$ of fluid for degenerate ${}_nS_l$ mode.
- d_xi_r.m: analytical radial derivative of $\xi_r(r)$.

2.3.3. Common lowest level routines

- P_lm.m: fully normalized $P_l^m(\cos(\theta))$ associated Legendre polynomial (= $p(\theta)$).
- d_P_lm.m: analytical theta derivative $q(\theta)$ of the fully normalized $P_l^m(\cos(\theta))$ associated Legendre polynomial.
- spherical_bessel_j.m: $j_l(x)$ spherical Bessel function of degree l of the first kind.
- spherical_bessel_y.m: $y_l(x)$ spherical Bessel function of degree l of the second kind.
- d_spherical_bessel_j.m: analytical derivative $dj_l(x)/dx$ of the spherical Bessel function of the first kind.
- d_spherical_bessel_y.m: analytical derivative $dy_l(x)/dx$ of the spherical Bessel function of the second kind.
- d2_spherical_bessel_j.m: analytical second derivative $d^2j_l(x)/dx^2$ of the spherical Bessel function of the first kind.
- d2_spherical_bessel_y.m: analytical second derivative $d^2y_l(x)/dx^2$ of the spherical Bessel function of the second kind.

3. Mode attenuation and synthetic spectra

From the theory discussed so far, we get the wave numbers and resonance frequencies of the acoustic modes, taking into account (in a linearized way) shell elasticity and ellipticity, global rotation, and differential fluid rotation. In order to produce synthetic spectra from these mode data, we need to predict the amplitude and shape of the spectrum around each resonance. We follow here the theory developped in Moldover et al. (1986) and Trusler (1991). The amplitude is controlled by the positions of the loudspeaker $(r_s, \theta_s, \varphi_s)$ and microphone $(r_r, \theta_r, \varphi_r)$ and the shape of the mode. The spectral amplitude ${}_n\mathcal{A}_l^m(f)$ of a given ${}_nS_l^m$ mode reads:

$$ {}_n\mathcal{A}_l^m = R(r_r)\, R(r_s)\, P_l^m(\cos\theta_r)\, P_l^m(\cos\theta_s)\, \cos m(\varphi_r - \varphi_s), \tag{26} $$

where $R(r)$ is the radial function of equation 4, to be evaluated at dimensionless radius unity if both the loudspeaker and the microphones are mounted flush at the outer boundary, as in ZoRo2.

3.1. attenuation mechanisms

The book of Trusler (1991) nicely discusses the attenuation mechanisms at work in gases. Viscous and thermal dissipation in the bulk contributes little to the attenuation of acoustic waves. It depends upon the kinematic viscosity ν_f of the fluid, its thermal diffusivity κ_f and its Gruneisen C_P/C_V index. The main attenuation mechanism occurs at the contact with the solid boundaries of the fluid. For isothermal boundaries (appropriate for metallic shells), the attenuation depends upon the same thermodynamic properties of the gas, but acting in the thin boundary layers forming at these frontiers. Following Moldover et al. (1986), we compute these contributions to the half-width ${}_ng_l$ of the spectral resonance peaks. We start from equation 42 of Moldover et al. (1986), which gives the bulk and boundary dissipation contributions g_{bulk} and $g_{boundary}$ to ${}_ng_l$, in the case of a rigid boundary. The boundary dissipation also slightly shifts the resonance peak by ${}_n\Delta f_l = -g_{boundary}$.

From equation 39 of Moldover et al. (1986) we get the bulk dissipation contribution as:

$$ g_{bulk} = \frac{{}_nk_l^2}{4\pi r_o^2}\left[(\gamma-1)\kappa_f + \frac{4}{3}\nu_f + \nu_{bulk}\right], \tag{27} $$

where we used ${}_nf_l/c = {}_nk_l/2\pi r_o$ (remember that the ${}_nk_l$ are dimensionless). The quantity ν_{bulk} is the bulk viscosity (kinematic here). Note that Moldover et al. (1986) have an erroneous 1/2 factor for that term, see Guianvarc'h et al. (2009) for example. The ratio ν_{bulk}/ν_f can be very different for different gases. Cramer (2012) computes this ratio for several gases as a function of temperature. At ambient temperature and low pressure, he finds that this ratio is of order 1 for N_2 and air, but is as large as 30 for H_2, 350 for SF_6 and 3500 for CO_2!

I have added bulk viscosity values for all fluids proposed in compute_modes_menu.m or gas_properties.m. Values are from Cramer (2012), or references therein, for gases; from Holmes et al. (2011) for water; from Awasthi and Murthy (1985) for liquid sodium.

The boundary dissipation occurs in the thin thermal and viscous boundary layers at the walls of the containers. The thickness of these boundary layers, respectively δ_T and δ_U, are given by equations 9 and 10 of Moldover et al. (1986):

$$ \delta_T = \sqrt{\frac{\kappa_f}{\pi_n f_l}} \tag{28} $$

$$ \delta_U = \sqrt{\frac{\nu_f}{\pi_n f_l}}. \tag{29} $$

Equation 42 of Moldover et al. (1986) then provides the $g_{boundary}$ contribution as:

$$ g_{boundary} = \frac{{}_nf_l}{2r_o}\frac{(\gamma-1)\,\delta_T + \frac{l(l+1)}{{}_nk_l^2}\,\delta_U}{1 - \frac{l(l+1)}{{}_nk_l^2}} \tag{30} $$

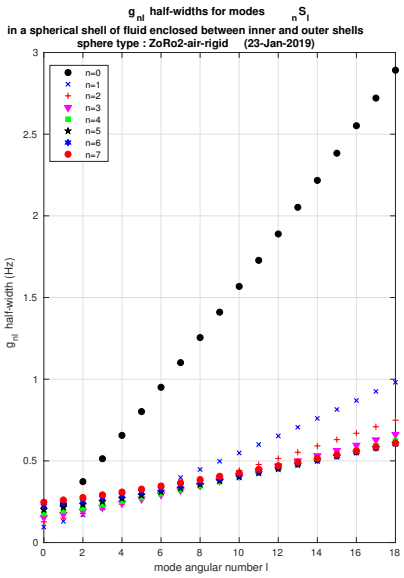

Figure 3: Half-widths ${}_ng_l$ of spectral resonance peaks for degenerate attenuated ${}_nS_l$ multiplets as a function of angular degree l and radial degree n in the ZoRo2 experiment filled with air, assuming a rigid outer wall.

In the end, the peak half-width is:

$$ {}_ng_l = g_{bulk} + g_{boundary}, \tag{31} $$

and the peak frequency shift is:

$$ {}_n\Delta f_l = -g_{boundary}. \tag{32} $$

Figure 3 shows the ${}_ng_l$ half-widths of spectral peaks in ZoRo2.

Note that the acoustic impedance of the walls of the container can also contribute to the attenuation and frequency shift. It is treated in Moldover et al. (1986).

3.2. resonance spectral shape

Including all the ingredients discussed so far, we get the expected resonance frequency ${}_nf_l^m$ of a given ${}_nS_l^m$ singlet as:

$$ {}_nf_l^m = {}_nf_l - m_nC_lf_o + {}_n\Delta_l^m + {}_n\delta_l^m + {}_n\Delta f_l^m, \tag{33} $$

where the right hand side terms are successively: the ideal multiplet mode frequency ${}_nf_l$ (equation 11), Coriolis splitting due to global rotation (equation 20), Doppler splitting ${}_n\Delta_l^m$ due to fluid differential rotation (equation 22), ellipticity splitting ${}_n\delta_l^m$ caused by ellipticity (presented in package Notes_ellipticity_pipeline), and frequency shift ${}_n\Delta f_l^m$ produced by attenuation at the boundaries (equation 32).

The spectrum of each individual singlet can be approximated as a Lorentzian (equation 3.1.1 of Trusler (1991)), as:

$$ spectrum(f) = \left| \frac{\mathrm{i}\,{}_n\mathcal{A}_l^m}{{}_ng_l + \mathrm{i}\left(f - {}_nf_l^m\right)} \right|. \tag{34} $$

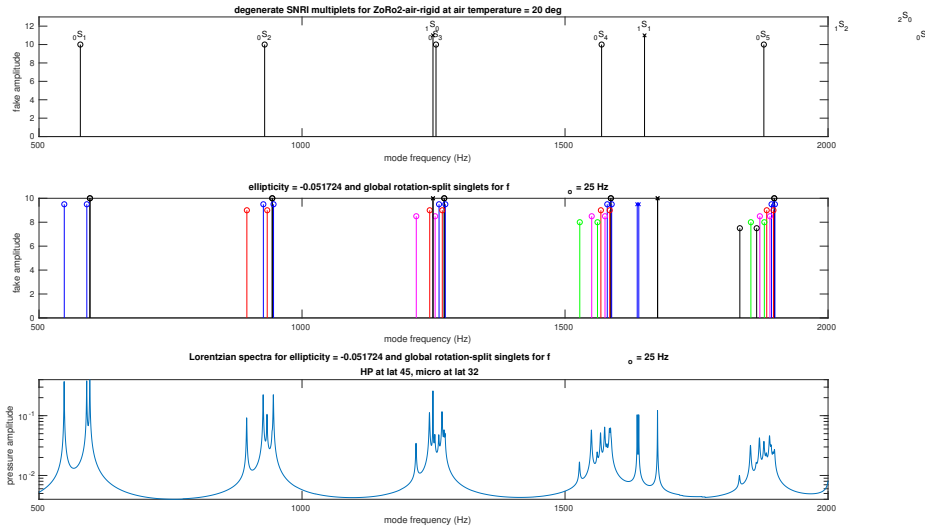

Figure 4: Zoom on an acoustic spectrum for ZoRo2 as a function of frequency, for a global rotation rate f_o = 25 Hz.

Figure 4 shows a zoom on a spectrum for ZoRo2.

The complete acoustic spectrum is obtained by summing all singlet contributions. It should be multiplied by the spectral transfer functions $Z_s(f)$ of the loudspeaker and $Z_r(f)$ of the microphone, if available.

3.3. matlab programs

3.3.1. matlab scripts

- draw_elliptic_rotation_spectra.m: in this script, one chooses a spherical mode file (such as 'ZoRo2-air-rigid') saved by the compute_modes_menu.m script. The script reads the mode file, and asks for an ellipticity and rotation values. It computes the mode splitting due to ellipticity and global rotation. Requesting loudspeaker and microphone latitudes, it computes the expected spectral amplitudes and builds a complete synthetic spectrum. Note that the spectral transfer functions and longitudes of the loudspeaker and microphone are not taken into account yet. In the same figure, it plots as a function of frequency:
  - the original degenerate spherical ${}_nS_l$ lines with their names,
  - the lines of the ${}_nS_l^m$ modes taking into account ellipticity (if any) and global rotation (if any),
  - the synthetic spectra built from these lines, taking into account mode attenuation and the source-receiver geometry.
- compare_ZoRo2_spectra.m: this script is based on the previous one and adds the reading and over-plotting of an experimentally obtained ZoRo spectrum. It includes the amplitude term connected to the difference in longitude between the loudspeaker

and the microphone (see equation 26). Temporarily, it also contains the retrieval and plot of an empirical transfer function $Z(f)$ in order to get similar amplitudes for the data and the synthetics.

3.3.2. matlab functions

- draw_attenuation_coefficients.m: plots the attenuation half-widths ${}_ng_l$ of the ${}_nS_l$ modes as a function of angular degree l for all available n.
- read_ZoRo_spectra.m: reads ZoRo '.txt' files as produced by Sylvie in January 2019.
- infos_install_ZoRo2.m: following the DTS philosophy, this function provides the coordinates (r, latitude, longitude) of a ZoRo2 element given its name (such as 'H01' or 'E04'), following the nomenclature established by Sylvie in January 2019 and the technical drawings of ZoRo2 by Max in 2018.

Most relevant functions are placed in the 'acoustic_library' folder.

- attenuation_half_width.m: computes the half-width ${}_ng_l$ of spectral peaks, and the corresponding resonance frequency shift ${}_n\Delta f_l$ for degenerate ${}_nS_l$ modes.
- build_Lorentzian.m: builds a Lorentzian spectrum for mode resonance at a given frequency, with a given half-width.

4. Conclusion

We now have a fairly complete set of simple tools to treat acoustic modes in our experiments. There are several additional developments that would be interesting:

- implementation of attenuation due to the impedance of the elastic walls.

References

Aerts, C., Christensen-Dalsgaard, J., Kurtz, D. W., 2010. Asteroseismology. Springer Science & Business Media.

Awasthi, O., Murthy, B., 1985. Bulk viscosity and ultrasonic attenuation in liquid metals. Physics Letters A 108 (2), 119–122.

Cramer, M. S., 2012. Numerical estimates for the bulk viscosity of ideal gases. Physics of fluids 24 (6), 066102.

Dahlen, F., 1976. Reply [to "comments on 'the correction of great circular surface wave phase velocity measurements from the rotation and ellipticity of the earth'by fa dahlen"]. Journal of Geophysical Research 81 (26), 4951–4956.

Dahlen, F., Tromp, J., 1998. Theoretical global seismology. Princeton university press.

Dahlen, F. A., 1968. The normal modes of a rotating, elliptical earth. Geophysical Journal International 16 (4), 329–367.

Guianvarc'h, C., Pitre, L., Bruneau, M., Bruneau, A.-M., 2009. Acoustic field in a quasi-spherical resonator: unified perturbation model. The Journal of the Acoustical Society of America 125 (3), 1416–1425.

Holmes, M., Parker, N., Povey, M., 2011. Temperature dependence of bulk viscosity in water using acoustic spectroscopy. In: Journal of Physics: Conference Series. Vol. 269. IOP Publishing, p. 012011.

Hu, H., Wang, Y., Wang, D., 2015. On the sound attenuation in fluid due to the thermal diffusion and viscous dissipation. Physics Letters A 379 (32-33), 1799–1801.

Jordan, P., Keiffer, R., 2016. Comments on: "on the sound attenuation in fluid due to the thermal diffusion and viscous dissipation" [phys. lett. a 379 (2015) 1799–1801]. Physics Letters A 380 (14), 1392 – 1393. URL http://www.sciencedirect.com/science/article/pii/S0375960116000931

Mehl, J. B., 2007. Acoustic eigenvalues of a quasispherical resonator: second order shape perturbation theory for arbitrary modes. Journal of research of the National Institute of Standards and Technology 112 (3), 163.

Moldover, M. R., Mehl, J. B., Greenspan, M., 1986. Gas-filled spherical resonators: Theory and experiment. The Journal of the Acoustical Society of America 79 (2), 253–272.

Rand, R., DiMaggio, F., 1967. Vibrations of fluid-filled spherical and spheroidal shells. The Journal of the Acoustical Society of America 42 (6), 1278–1286.

Triana, S. A., Zimmerman, D. S., Nataf, H.-C., Thorette, A., Lekic, V., Lathrop, D. P., 2014. Helioseismology in a bottle: modal acoustic velocimetry. New Journal of Physics 16 (11), 113005.

Trusler, M., 1991. Physical acoustics and metrology of fluids. CRC Press.